ACS chemical biology

ARTICLES

pubs.acs.org/acschemicalbiology

Structural Basis for Inhibiting β-Amyloid Oligomerization by a Non-coded β-Breaker-Substituted Endomorphin Analogue

Anat Frydman-Marom,[†] Marino Convertino,[‡] Riccardo Pellarin,[‡] Ayala Lampel,[†] Ronit Shaltiel-Karyo,[†] Daniel Segal,[†] Amedeo Caflisch,[*,‡] Deborah E. Shalev,[*,§] and Ehud Gazit[*,†]

[†]Department of Molecular Microbiology & Biotechnology, Tel-Aviv University, Tel-Aviv 69978, Israel

[‡]Department of Biochemistry, University of Zurich, CH-8057 Zurich, Switzerland

[§]Wolfson Centre for Applied Structural Biology, Hebrew University of Jerusalem, Safra Campus, Givat Ram, Jerusalem 91904, Israel

Supporting Information

ABSTRACT: The distribution of endomorphins (EM) 1 and 2 in the human brain inversely correlates with cerebral neurodegeneration in Alzheimer's disease (AD), implying a protective role. These endogenous opioid peptides incorporate aromatic residues and a β-breaker motif, as seen in several optimized inhibitors of Aβ aggregation. The activity of native endomorphins was studied, as well as the rationally designed analogue Aib-1, which includes a remarkably efficient β-breaker, α-aminoisobutyric acid (Aib). *In vitro* and GFP fusion protein assays showed that Aib-1 interacted with Aβ and markedly inhibited the formation of toxic oligomer and fibril growth. Moreover, Aib-1 prevented the toxicity of Aβ toward neuronal PC12 cells and markedly rectified reduced longevity of an AD fly model. Atomistic simulations and NMR-derived solution structures revealed that Aib-1 significantly reduced the propensity of Aβ to aggregate due to multimode interactions including aromatic, hydrophobic, and polar contacts. We suggest that hindering the self-assembly process by interfering with the aromatic core of amyloidogenic peptides may pave the way toward developing therapeutic agents to treat amyloid-associated diseases.

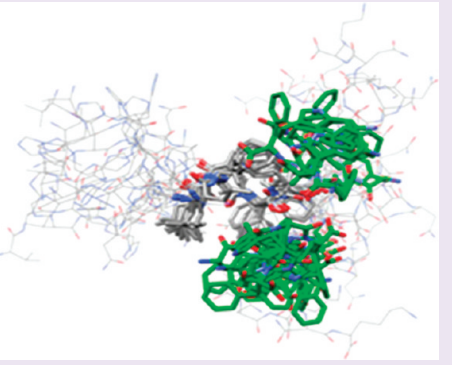

Alzheimer's disease (AD), the most widespread cause of dementia in the elderly population, is the sixth leading cause of death in the United States.[1] Strong genetic, physiological, and biochemical evidence suggests that the β-amyloid polypeptide (Aβ) plays a key role in the pathogenesis of the disease.[2] Although the etiologic role of Aβ in AD is acknowledged,[3] the molecular mechanism of neurotoxicity is still under debate. The occurrence of insoluble Aβ fibrils in AD has long been recognized, yet neuronal damage in AD may occur in the absence of amyloid plaques. Recent studies have demonstrated that nonfibrillar structures, including oligomers (56 kDa),[4,5] amyloid-derived diffusible ligands (ADDLs),[6] and protofibrils,[7] possess neurotoxic properties. Because the process of amyloid assembly is accompanied by a transition of a correctly folded monomer into oligomers and/or fibrils even at low, submicromolar concentrations, a very precise and highly specific process of molecular recognition must occur to enable such well-ordered, supramolecular structures to be formed.[8]

Rational drug design approaches for developing inhibitors of Aβ aggregation are hampered by the absence of specific structural information on soluble or fibrillar Aβ, whose amorphic nature precludes using most structural methods. Previous experimental and theoretical studies by our group and others have indicated the apparent role of aromatic residues in the molecular recognition and self-assembly processes that lead to the formation of amyloid fibrils.[9−13] The aromatic amino acid tryptophan has been found to be very important for facilitating protein−protein interactions[14] and was ranked as the amino acid with the highest amyloidogenic propensity.[15] Thus, inhibiting Aβ aggregation using aromatic entities, with an emphasis on tryptophan, is a rational strategy for therapeutic intervention in AD.[16] A number of small aromatic molecules such as short peptides,[17,18] polyphenols,[19] indole derivatives,[20] and quinines[21,22] have been shown to inhibit aggregation of several amyloidogenic peptides.

Moreover, conjugating a β-breaker motif to recognition elements has been proposed to hinder amyloid formation.[23] A milestone in the search for proof of this concept was provided by Soto *et al.*, who demonstrated that amyloid formation was inhibited by incorporating proline as a β-breaker element in short peptides bearing a recognition sequence of the amyloidogenic protein.[23] Our approach for breaking amyloidogenic β-sheet structures utilizes α-aminoisobutyric acid (Aib) as a potent β-breaker element.[16,24] This achiral amino acid has two methyl residues attached to the Cα atom and strongly favors helical conformations. The Ramachandran plot clearly demonstrates that Aib has a significantly higher potential to serve as a β-breaker than proline.[24]

While the β-breaker strategy has been suggested to inhibit mature fibril formation, it may also be valid for inhibiting the early

Received: March 24, 2011
Accepted: September 5, 2011
Published: September 05, 2011

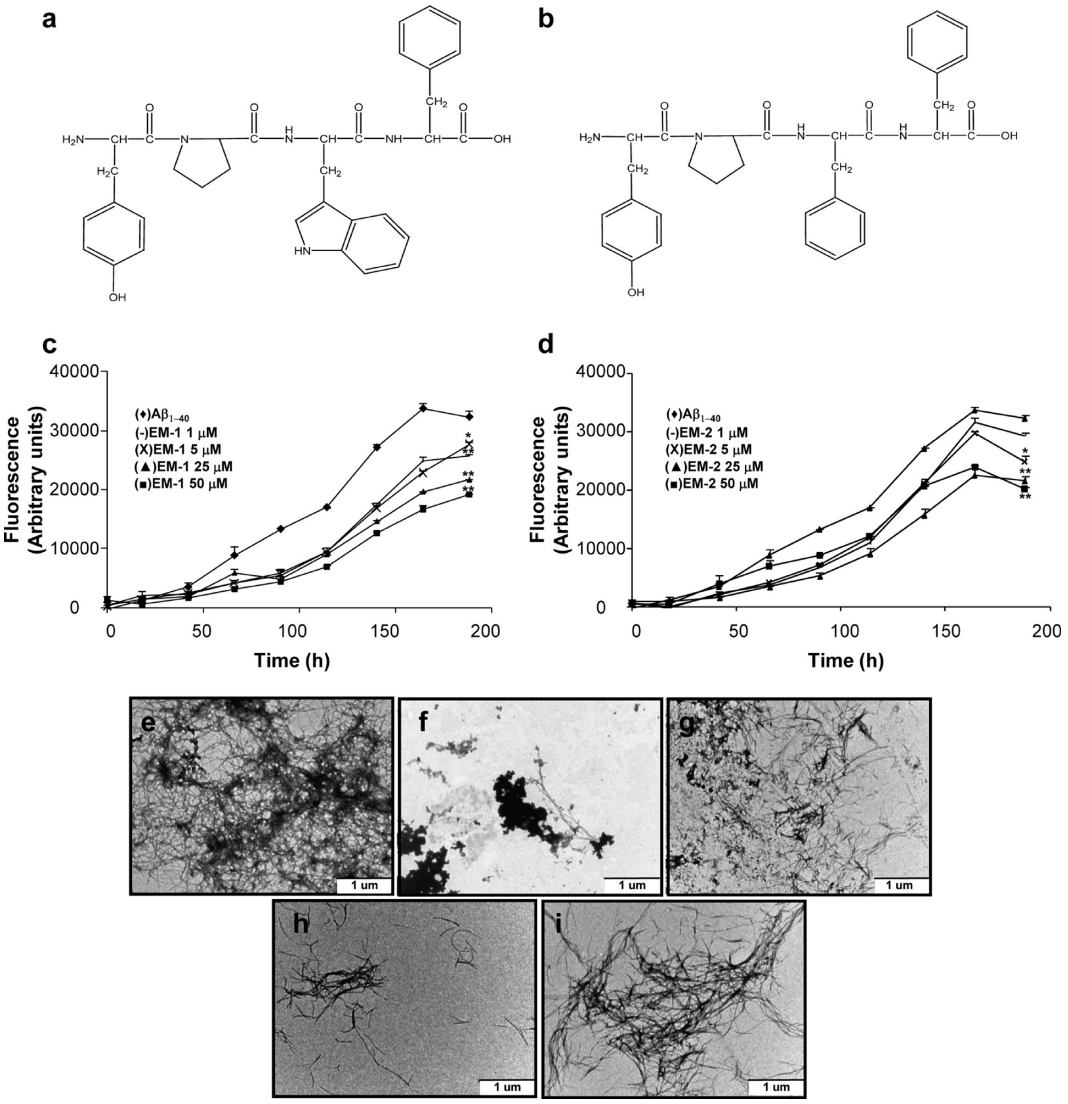

Figure 1. Inhibition of Aβ fibril formation by EM-1 and EM-2. Schematic representation of (a) EM-1 (Tyr-Pro-Trp-Phe) and (b) EM-2 (Tyr-Pro-Phe-Phe). (c, d) The kinetics of Aβ_{1-40} fibril formation in the presence or absence of (c) EM-1 or (d) EM-2 as assessed by the Thioflavin-T biding assay over the course of 200 h. Concentrations of the inhibitors are indicated in the graph; control is Aβ_{1-40} (5 μM). (e−i) Transmission electron microscope images taken from ThT analysis after 200 h: (e) Aβ_{1-40} alone, (f) Aβ_{1-40} with EM-1 50 μM, (g) Aβ_{1-40} with EM-1 1 μM, (h) Aβ_{1-40} with EM-2 50 μM, (i) Aβ_{1-40} with EM-2 1 μM. Scale bar is 1 μm. * Pv < 0.05, ** Pv < 0.005.

intermediates that are also rich in β-sheet structures.[16] We previously demonstrated that Aβ oligomerization was efficiently inhibited by a short dipeptide, D-Trp-Aib, both *in vitro* and *in vivo*. Treatment with this novel compound restored the level of cognitive performances in AD-model mice to that of nontransgenic ones.[16]

Endomorphin-1 (EM-1; Tyr-Pro-Trp-Phe) and endomorphin-2 (EM-2; Tyr-Pro-Phe-Phe) are two endogenous opioid peptides that are widespread in the human central nervous system.[25] Neither endomorphin is found in the hippocampus, which suffers most from massive cell loss in AD pathology.[25,26] Szegedi and co-workers were the first to theorize that EM-2 might possess some protective activity against Aβ_{1-42} because of its high structural similarity with the Sotòs peptide, Leu-Pro-Phe-Phe-Asp (LPFFD).[27,28] There is a high degree of similarity between the sequences of the two endomorphins and our rationally designed molecule, D-Trp-Aib, in terms of aromaticity and β-breaker motifs.[16]

A novel peptide (termed Aib-1) was designed based on the sequence of the natural EM-1 with an Aib residue instead of proline, to improve affinity toward Aβ and increase the β-breaker potential.[16,24] The designed peptide showed enhanced affinity toward Aβ over EM-1 and hindered Aβ aggregation into toxic oligomers and fibrils both experimentally and in implicit solvent molecular dynamics (MD) simulations. NMR-derived solution structures showed aromatic, hydrophobic, and polar interactions between Aib-1 and a truncated β-amyloid peptide model, which presumably reduced the propensity of Aβ to aggregate with increased efficiency due to the multimode nature of the interaction. Moreover, *ex vivo* and *in vivo* experiments demonstrated that Aib-1 significantly meliorated the viability and life span deficiencies of an established AD *Drosophila* fly model.

RESULTS AND DISCUSSION

Endogenous EM-1 and EM-2 Inhibit Aβ Aggregation. Natural endogenous molecules (EM-1 and EM-2) (Figure 1a,b) were found to be surprisingly similar to our rationally designed

library of inhibitor peptides that contain aromatic moieties in addition to β-sheet breaker elements.[16] Moreover, EM-2 was reported to possess protective properties against $A\beta_{1-42}$-induced attenuation of cell redox activity and neuromodulation *in vitro* and *in vivo*.[28] Thus, we tested their inhibitory potentials using the thioflavin-T (ThT) binding assay to provide quantitative information on amyloid fibril growth. The amount of $A\beta_{1-40}$ fibrils was measured after adding a fixed concentration of each compound. Both peptides inhibited fibrillization to some extent: the maximum inhibition by EM-2 was around 30% and by EM-1 was around 50% at the same peptide concentration (Figure 1c,d).

Inhibition of $A\beta_{1-42}$ fibrillization was tested as well. The $A\beta_{1-42}$ peptide is the major component of senile plaques, and the ratio of $A\beta_{1-42}/A\beta_{1-40}$ was found to be increased in AD patients' brains.[29] The results clearly showed a pattern of dose-dependent inhibition. The IC_{50} of each inhibitor was calculated, and apparent IC_{50} values of 30 μM and 60 μM were determined for EM-1 (Supporting Information S1a) and EM-2 (data not shown), respectively.

Ultrastructural Analysis of Aggregation. The inhibitory effect of the compounds on the ultrastructural properties of the assembled Aβ was determined using transmission electron microscopy (TEM) analysis. Samples of $A\beta_{1-40}$ from the kinetic assay after incubation for 6 days formed large and branched fibrils (Figure 1e). Samples of $A\beta_{1-40}$ containing 1 μM EM-1 (Figure 1g) and 1 μM EM-2 (Figure 1i) showed aggregates similar to those observed in the control sample but in smaller amounts, whereas the $A\beta_{1-40}$ sample containing 50 μM EM-1 (Figure 1f) contained only negligible amounts of short fibrils. Thin, low-density small fibrils were observed in the sample containing $A\beta_{1-40}$ and 50 μM EM-2 (Figure 1h), compared to the fibrils formed by Aβ protein alone. These results highly correlate with the results of the ThT assay.

Characterization of the Affinity between EM-1 and Aβ. Changes in the intrinsic fluorescence polarization values of the Trp-fluorophore were monitored to determine the affinity of EM-1 and the early $A\beta_{1-42}$ assemblies, taking advantage of the relatively small size of EM-1 relative to that of $A\beta_{1-42}$ oligomers. Increasing amounts of early assemblies of $A\beta_{1-42}$ were titrated into a solution of EM-1, and anisotropy was determined (Supporting Information S2a). The calculated affinity constant was ~2 μM. This suggests that the tryptophan of EM-1 mediates the interaction with Aβ, giving an interaction stronger than that of EM-2, resulting in better inhibition. This correlates well with our previous results, in which a dipeptide containing Phe was less potent inhibitor of oligomer formation than the same peptide with a Trp substitution.[16] Moreover, an unbiased analysis using peptide array technology has shown a significantly higher affinity of the tryptophan-modified recognition module in the molecular association of islet amyloid polypeptide.[30,31] The efficient inhibition of Aβ fibrillization by these endomorphins is consistent with the findings that brain areas deficient in these peptides, such as the hippocampus, are severely affected in both AD patients and transgenic animals,[28] suggesting a possible role for the endogenous tetrapeptide in the area-selective neuronal loss seen in AD.

A Derivative Molecule, Aib-1, Dramatically Reduced Aβ Aggregation. Endomorphins cannot serve as direct therapeutic agents for AD since elevated levels may result in undesired side effects including focal epileptic seizures. Nevertheless, their sequence may serve as a basis for designing inhibitors that may efficiently arrest Aβ aggregation without activating the μ-opioid receptor.

The Aib residue has been shown to have a high tendency to induce helical conformations and to disrupt β-sheet structures in a large variety of peptides.[32] Incorporating Aib into a fully protected Alzheimer's Aβ fragment (residues 17−21) was shown to induce a helical structure of the fragment in organic solvents.[33] We have previously used Aib as a conjugated β-breaker element for inhibiting hIAPP amyloid fibril formation[24] and also designed a dipeptide containing Trp and Aib (D-Trp-Aib) that combined properties of aromatic recognition interfaces with β-breakage strategy: D-Trp-Aib significantly reduced the amount of amyloid deposits in the brain of AD transgenic mice models and improved their cognitive performances.[16] The proline residue of EM-1 was substituted by Aib resulting in the Aib-1 peptide (Tyr-Aib-Trp-Phe) (Figure 2a). The recognition surface of the modified peptide was virtually identical to that of the native sequence. The interaction between Aib-1 and $A\beta_{1-42}$ gave a calculated affinity constant of ~800 nM (Supporting Information S2b), showing Aib-1 interacts with Aβ better than EM-1. The ThT binding assay of $A\beta_{1-40}$ in the presence or absence of different excess concentrations of Aib-1 showed that the amyloid fibril formation was significantly reduced in the presence of the Aib-1 peptide, as reflected in fluorescence intensities (Figure 2b,c). This inhibition was dose-dependent, where the maximum percentage of inhibition was ~70%. IC_{50} for the Aib-1 molecule was determined as 5 μM (Supporting Information S1b).

The morphology of samples from the ThT experiment was observed by TEM. Hardly any fibrillar structures could be detected in the $A\beta_{1-40}$ samples containing 50 μM Aib-1, even after a long incubation period (Figure 2e). Extremely low-density amyloid fibrils were observed in samples containing $A\beta_{1-40}$ with 0.5 μM Aib-1 (Figure 2f) compared to the high abundance of ordered fibrillar structures that were observed in samples containing $A\beta_{1-40}$ alone (Figure 2d).

Inhibiting Toxic Oligomer Species by EM-1 and Aib-1. Recent evidence indicates that the toxicity of Aβ and other amyloidogenic peptides lies in their soluble oligomeric forms.[4−6,34,35] This claim is supported by many *in vitro* and *in vivo* studies, suggesting that potential antiamyloid compounds should aim at blocking the very early stages of amyloid oligomerization.[16,36−38] The potential of our compounds to inhibit oligomer formation was tested using SDS-stable oligomers, which display toxic effects on the long-term potentiation of cultured neural cells according to Hillen and co-workers.[4] EM-1 and Aib-1 were each incubated with $A\beta_{1-42}$ at increasing molar ratios, and the reaction mixtures were loaded on SDS-PAGE followed by Western blot analysis with 6E10 antibody (Figure 3a). A 10-fold excess of EM-1 significantly inhibited the formation of the 56 kDa (56*) toxic oligomers, in comparison with Aib-1, which already exhibited the same inhibitory effect at a molar ratio of 1:1. Aib-1 seems to efficiently prevent the early nontoxic oligomers from developing into the toxic species.

Fluorescent Screen for Inhibitors of Aβ Aggregation. $A\beta_{1-42}$ aggregation was followed by another unbiased technique developed by Kim *et al.* that uses $A\beta_{1-42}$ fused to GFP protein.[39] Since GFP folding into its native fluorescent structure occurs slowly,[40] misfolding and aggregation of the fused $A\beta_{1-42}$ sequence may cause the entire $A\beta_{1-42}$-GFP fusion protein to misfold before it can correctly fold into its fluorescent structure. Compounds that inhibit $A\beta_{1-42}$ aggregation permit GFP to fold into its native structure, which can be identified by the resulting fluorescent signal. *E. coli* cells expressing the $A\beta_{1-42}$-GFP fusion protein were dispensed into 96-well plates. EM-1 and Aib-1 were added to each well at different concentrations, and $A\beta_{1-42}$-GFP fusion protein expression was induced by adding isopropyl-β-D-thiogalactopyranoside

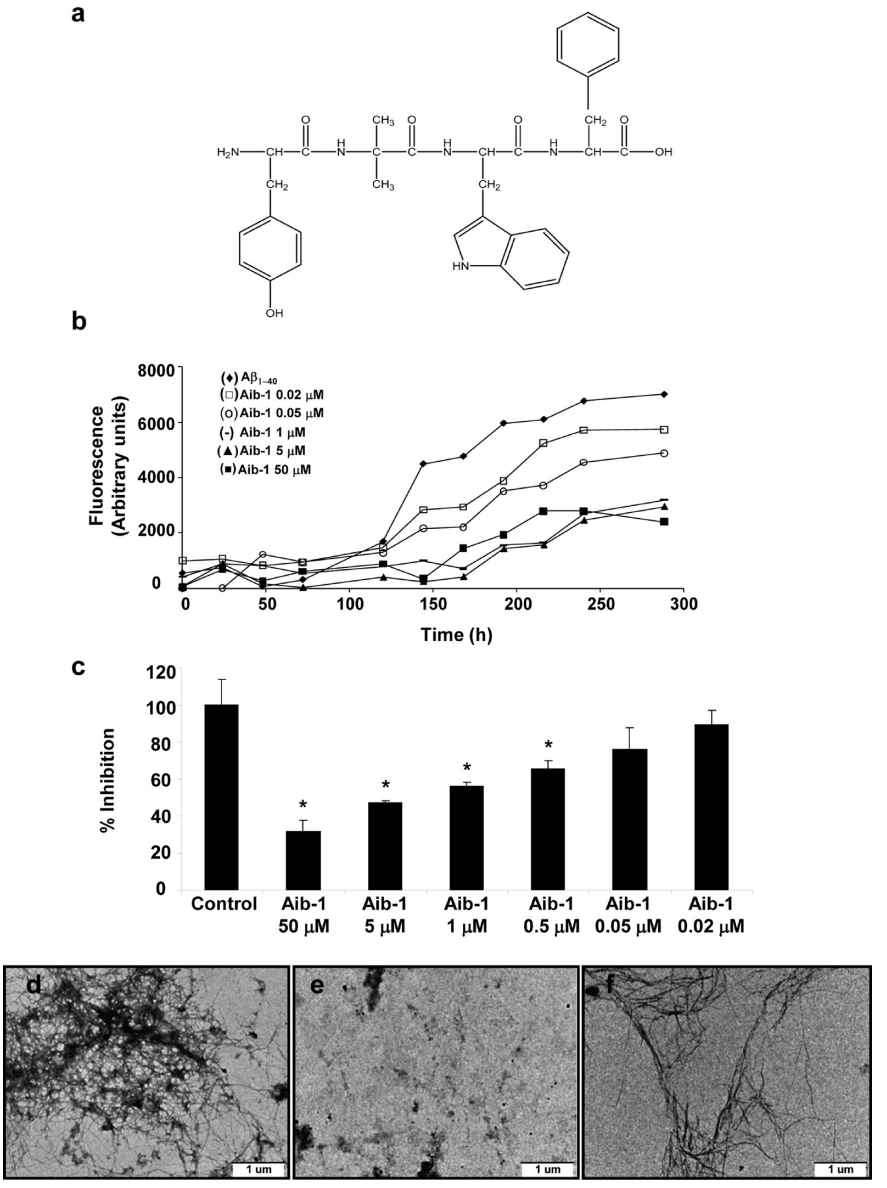

Figure 2. Inhibition of Aβ fibril formation by Aib-1. (a) Schematic representation of Aib-1 (Tyr-Aib-Trp-Phe). (b) ThT analysis of the percent of inhibition during 300 h. Concentrations of Aib-1 are indicated in the graph; control is Aβ_{1-40} (5 μM). (c) End point of ThT analysis measurement at T = 300 h. Concentrations are indicated in the figure. (d) TEM image of Aβ_{1-40} alone. (e) TEM image of Aβ_{1-40} with Aib-1 50 μM taken from ThT analysis after 200 h. (f) TEM image of Aβ_{1-40} with Aib-1 0.5 μM taken from ThT analysis after 200 h. Scale bar is 1 μm. * Pv < 0.05.

(IPTG). Following 3 h of induction, the fluorescence of each well was measured using a plate reader. The same volume of DDW was used as a negative control, and a GFP protein fused to an Aβ_{1-42} sequence containing a mutation that inhibits aggregation was used as a positive control.[41] Samples containing Aβ_{1-42}-GFP showed the lowest fluorescence, indicating aggregation, whereas wells containing EM-1 and Aib-1 at different concentrations presented dose-dependent fluorescence values (Figure 3b). The ability of Aib-1 to inhibit Aβ_{1-42} aggregation was slightly greater than that of EM-1. Importantly, the addition of the inhibitors (100 μM) to the positive control did not reduce the fluorescence (data not shown). A direct correlation between the fluorescent screen assays and the ThT, TEM, and oligomer assays was evident.

Aib-1 Inhibits the Cytotoxic Effect of Aβ toward PC12 Cultured Cell Line. In order to test the physiological relevance of Aib-1 and its potential to serve as AD treatment, we examined whether Aib-1 could inhibit Aβ-mediated cytotoxicity on the rat neuronal PC12 cell line. A control experiment showed that on its own, Aib-1 is not toxic to the cultured cells up to the concentration tested of 2 mM (data not shown). In contrast, Aβ_{1-42} oligomers were highly toxic to these cells (Figure 3c), which exhibited viability of 20% relative to untreated cells. Remarkably, when incubated with Aβ_{1-42} oligomers, Aib-1 displayed a dose-dependent reduction of the cytotoxic effect of Aβ_{1-42} oligomers, with cell viability restored to nearly 90% at Aβ_{1-42}/Aib-1 concentration ratio of 1:15 (Figure 3c). Similar results were also obtained when Aβ_{1-42} fibrils were incubated with the cells, where a low Aib-1 concentration (10 μM) exhibited complete restoration of cell viability (see Supporting Information S3).

***In Vitro* Assay of Peptide Stability.** A major drawback of using peptides as drugs for treating neurological diseases is their rapid metabolism by proteolytic enzymes.[42] Although Aib-1 was

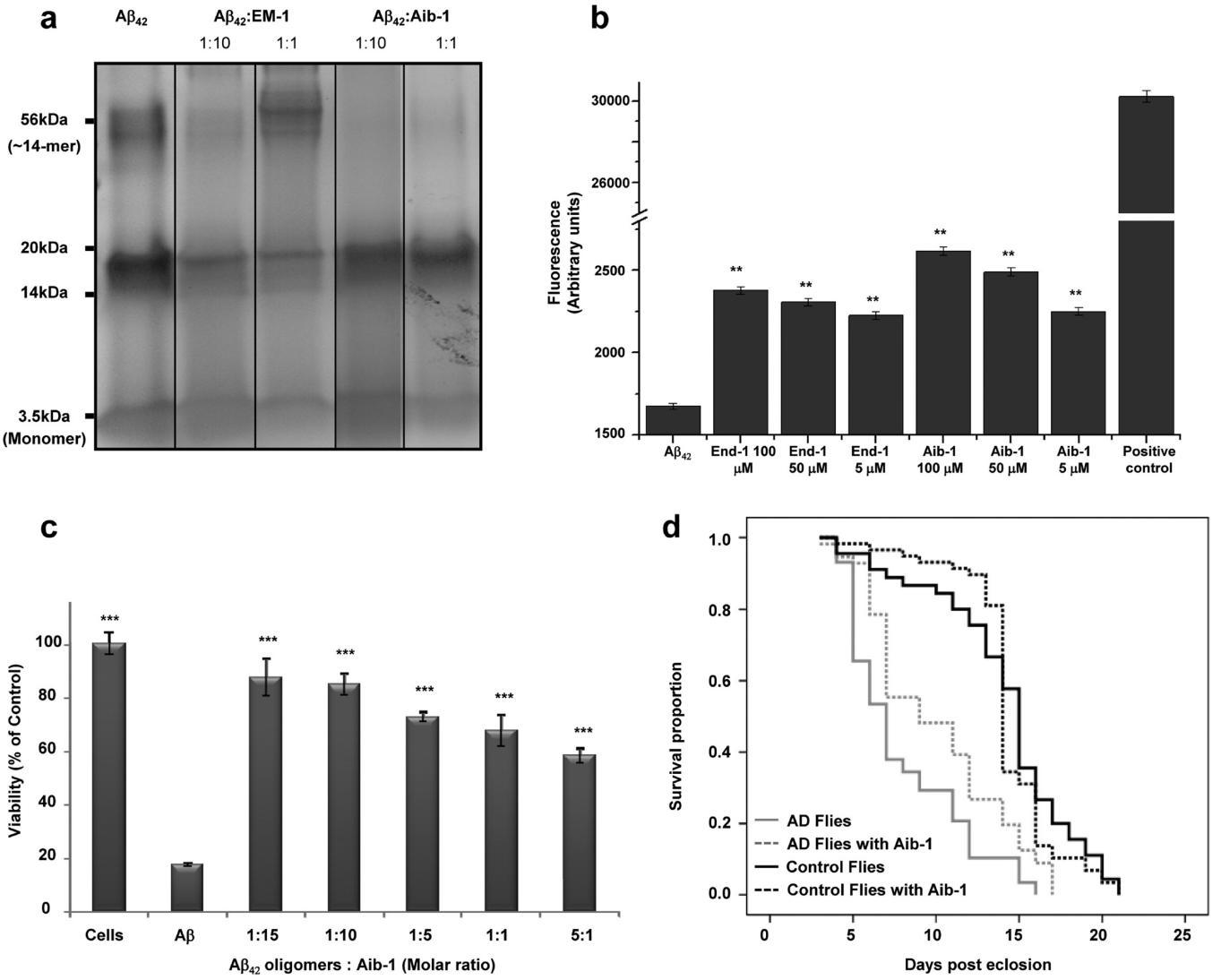

Figure 3. Aib-1 alleviates toxic effects of Aβ *in vitro* and in cell and fly assays. (a) Determining a dose-dependent effect of EM-1 and Aib-1 on soluble oligomer formation. Soluble oligomers were prepared in the presence or absence of increasing concentrations of EM-1 and Aib-1. Molar ratios of EM-1/Aib-1:Aβ_{1-42} are indicated in the figure. Control is Aβ_{1-42} (133 μM) alone. (b) Fluorescence-based screen using the Aβ_{1-42}-GFP fusion; negative control is the Aβ_{1-42} alone, positive control is a nonaggregative Aβ mutant-GFP fusion protein. Concentrations of the inhibitors EM-1 and Aib-1 are indicated. ** Pv < 0.01. (c) Aib-1 alleviated toxic effects of Aβ oligomers toward PC12 cell line. Samples of Aβ_{1-42} oligomers (5 μM) with or without various concentrations of Aib-1 were incubated for 24 h with PC12 cells culture. Cells viability was determined using the MTT viability assay. *** Pv < 0.001. (d) The effect of Aib-1 (D-amino acids) on longevity of AβArc42-expressing flies. The life span of four classes of flies ($n \approx 60$ in each group) was evaluated: AD flies grown on regular medium (gray line), AD flies grown on medium containing Aib-1 (gray dashed line), Control flies grown on regular medium (black line), Control flies grown on medium containing Aib-1 (black dashed line).

initially designed to improve the inhibition potential of the peptide, it also dramatically improved the peptide's stability.[43] The resistance of EM-1 and Aib-1 to enzymatic degradation was determined *in vitro* by incubating them for a period of 2 h in a fresh mouse-brain homogenate to model degradation in blood and tissues.[44] The results show that EM-1 was totally degraded by 2 h, while Aib-1 was still stable at that time (Supporting Information S4).

Effect of Aib-1 in an *in Vivo* Transgenic Fly System. Although Aib-1 exhibited dramatic abilities in the *in vitro* and cell culture, we wished to examine the effect of Aib-1 *in vivo*, in the context of the intact animal, using an established *Drosophila* model of AD. The model that was used overexpressed the Arctic (Arc) (E22G) mutant form of Aβ, *via* the Gal4-UAS system.[45] The arctic mutation is associated with enhanced Aβ protofibril formation and early onset familial AD.[46] Crossing female flies carrying the pan-neuronal elav-Gal4 driver to males carrying the UAS-regulated arctic (Arc) (E22G) mutant form transgene results in F1 AD flies expressing the Arc mutation in their nervous system. This fly model is very aggressive, displaying characteristic symptoms that include impaired locomotion and memory that decline with age, as well as markedly reduced longevity.[45] We fed the AβArc$_{42}$ flies either on regular *Drosophila* medium or medium supplemented with 0.75 mg/mL Aib-1 (D-amino acids) from the beginning of their larval stage through adulthood, and each class of adult offspring was monitored daily for survival.[38,45]

As reported, flies expressing the AβArc$_{42}$ mutation in their brain showed a markedly reduced life span compared to the

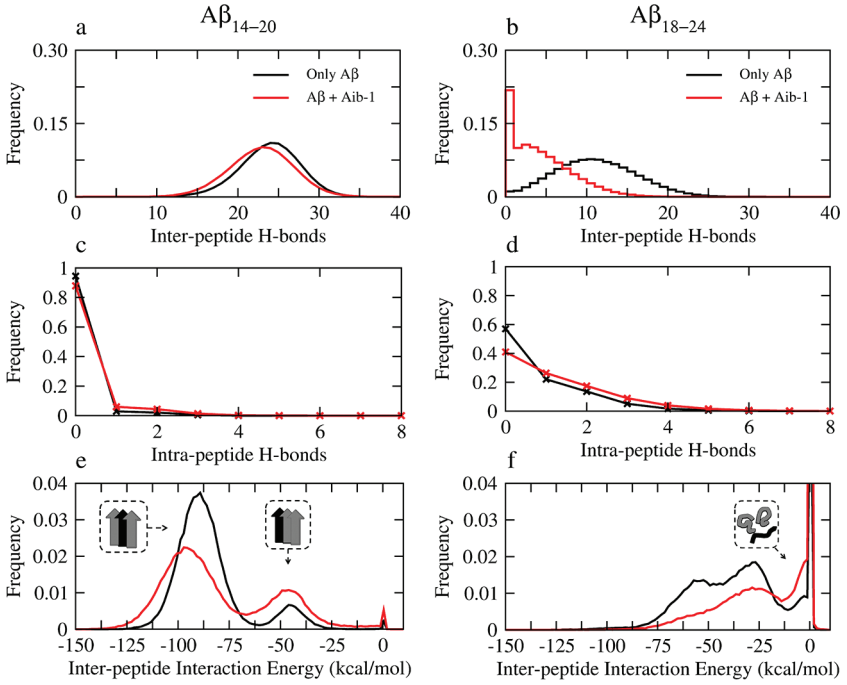

Figure 4. Effect of Aib-1 on the aggregation of the central segment of Aβ as observed in MD simulations of eight Aβ_{14-20} heptapeptides (left) and eight Aβ_{18-24} heptaptides (right). The interpeptide interaction energy (van der Waals plus electrostatic) of a single Aβ heptapeptide with the remaining seven heptapeptides, was evaluated separately in the presence and absence of Aib-1 and averaged over all heptapeptides. The distributions of interpeptide backbone H-bonds (a, b), intrapeptide backbone H-bonds (c, d), and interpeptide interaction energy (e, f) are shown. The differences in the distributions in the presence (red) and absence (black) of Aib-1 indicate that Aib-1 hinders the early phase of Aβ aggregation. In panels e and f, the insets show schematic illustrations of the position of the reference heptapeptide in the β-sheet aggregate and in the disordered system, respectively. In panel f, the frequency for fully separated peptides (data points at $x = 0$) is 0.07 and 0.25 for only Aβ and Aβ/Aib-1, respectively.

control flies (offspring that carried the Arc mutation transgene but did not express it because they lacked the Gal4 driver) (Figure 3d). The Aib-1 diet markedly rectified the reduced longevity of the AβArc$_{42}$ flies (Pv = 0.003) (Figure 3d). In contrast, Aib-1 had no significant effect on the life span of the control flies. These results show a specific and marked phenotypic recovery of the AβArc$_{42}$ flies fed with Aib-1 diet, suggesting that Aib-1 may serve as potential AD therapeutic agent.

Atomistic Simulations of the Influence of Aib-1 on Aβ Assembly. Implicit solvent[47] molecular dynamics (MD) simulations were carried out using CHARMM[48] to study the effects of Aib-1 on the early phase of Aβ aggregation. The influence of Aib-1 on the Aβ self-assembly process was investigated by focusing on segment 14−24 as in a previous combined experimental/simulation study.[21] This short segment is known to have a high β-aggregation propensity according to biophysical experiments[49] as well as atomistic simulations[50] and a phenomenological model based on physicochemical properties of the amino acid sequence.[51] A divide-and-conquer approach was adopted to efficiently sample conformational space.[50] The segment 14−24 was divided into two overlapping heptapetides Aβ_{14-20} and Aβ_{18-24}. The MD simulations were carried out using eight copies of Aβ_{14-20} or Aβ_{18-24} in the presence and absence of one Aib-1 molecule. At the start of each MD run, the eight peptides and the inhibitor were completely dissociated.

The number of interpeptide backbone hydrogen bonds (H-bonds) was used as a measure of the β-sheet aggregation propensity of the system. Figure 4 shows that Aβ_{14-20} had a higher propensity to form β-sheet aggregates than Aβ_{18-24}, in agreement with a previous simulation study that employed a different implicit solvent model.[50] During the MD simulations in the absence of Aib-1, the eight Aβ_{14-20} peptides were strongly associated, forming cross-β interactions with variable orientations and arrangements of the peptide chains. The simulations mainly explored two kinds of oligomeric structures: either a pair of four-stranded β-sheets associated through side-chain contacts or an eight-stranded β-sheet with fully parallel or mixed orientations of the strands. In contrast, the Aβ_{18-24} system only transiently associates with very low β-sheet content. Both Aβ peptide segments showed very frequent packing of the F19 and F20 side chains due to aromatic interactions among the phenyl rings. In the β-sheet(s) structures of Aβ_{14-20} the parallel stacking of F19 side chains and the stacking of F20 side chains stabilized the in-register β-parallel arrangement as in previous simulations of the heptapeptide segment GNNQQNY of the yeast prion protein Sup35.[52] Visual inspection of the MD runs with Aib-1 revealed a rather transient, fluid-like association of Aib-1 to the multiple β-sheet arrangements of the Aβ heptapeptides. The effect of Aib-1 on β-sheet aggregation of the Aβ_{14-20} and Aβ_{18-24} peptides was quantified by comparing the backbone H-bonds in the presence or absence of Aib-1 (Figure 4a−d), revealing that Aib-1 was able to interact with Aβ_{14-20} and Aβ_{18-24}, diminishing their ability to aggregate into ordered β-sheet structures. This effect of Aib-1 was evident in the reduced number of backbone H-bonds among the Aβ heptapeptides, as well as the increased number of intrapeptide H-bonds (Figure 4). Moreover, the influence of Aib-1 seemed more pronounced on Aβ_{18-24} than Aβ_{14-20}, due to the lower aggregation propensity of the former. As a consequence of the presence of Aib-1, the interaction energy between Aβ heptapeptides was less favorable

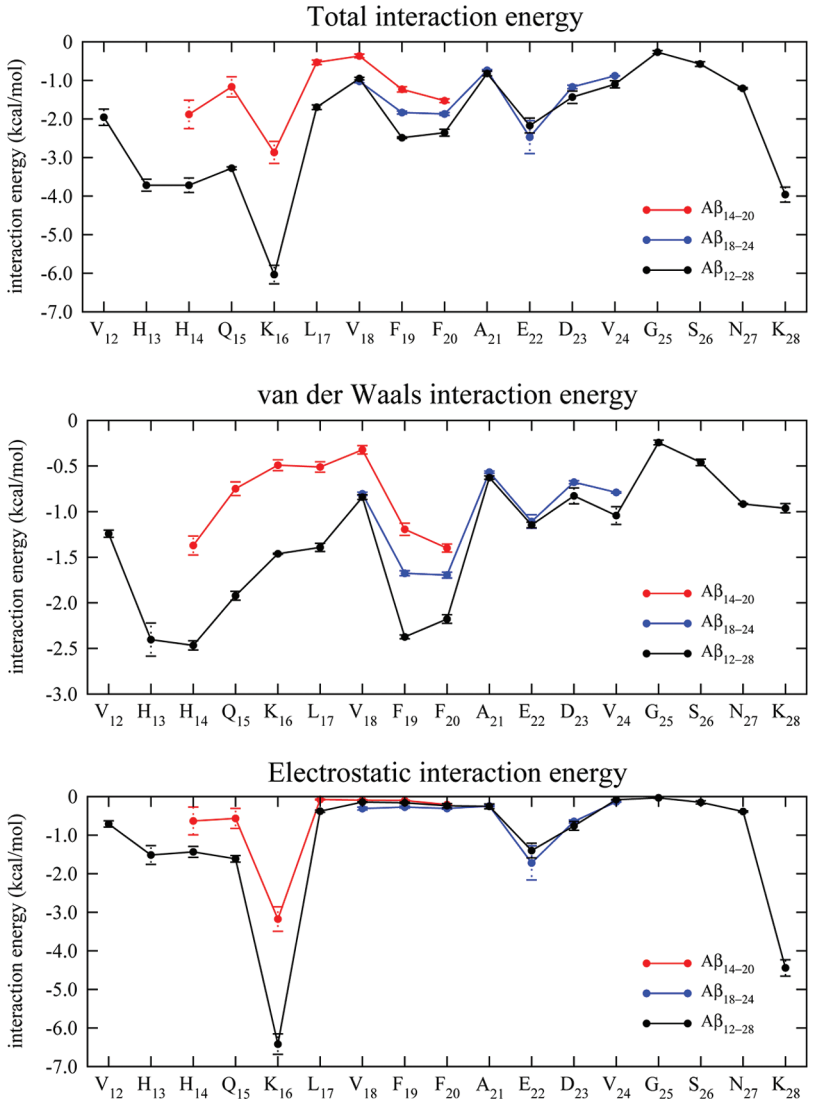

Figure 5. Profile of the interaction energy between Aib-1 and individual residues (backbone and side chain atoms) of Aβ_{12-28} (black), Aβ_{14-20} (red), and Aβ_{18-24} (blue). The error bars were obtained by block averaging over independent MD runs, *i.e.*, three 5-μs blocks for monomeric Aβ_{12-28} (black) and ten 2-μs blocks for each of the two octameric Aβ heptapeptide systems (red and blue).

on average, mainly because of a reduction of the number of strands in the β-sheets. The Aib-1 effect on the Aβ_{14-20} and Aβ_{18-24} segments is also seen in the interpeptide interaction energy that shows two peaks corresponding to a peptide within, and at the edge of, a parallel β-sheet (Figure 4e,f). In the presence of Aib-1, the former peak decreased, whereas the latter increased as a result of the decrease in the average number of strands in the β-sheet(s). It is important to note that these results were obtained from a statistically converged sampling as indicated by a block averaging analysis (Supporting Information S5).

Despite the nonspecific association of Aib-1 to Aβ oligomers, there is a large variability of interaction strength between Aib-1 and individual residues of Aβ. In particular, the interaction energy analysis revealed favorable van der Waals interactions with H13, H14, F19, and F20 side chains and electrostatic interactions with the side chains of K16, K28, and E22 (Figure 5). It must be stressed that the latter interactions are specific, and the favorable electrostatic energy is not solely due to the fact that Lys and Glu side chains bear charged groups, because the interactions with E22 are more favorable than with D23, and those with K16 are more favorable than with K28. Moreover the Aβ_{12-28}/Aib-1 interaction energy analysis shows similar interaction patterns as for the octameric heptapeptide systems (Figure 5) with slightly larger deviations for the Aβ_{14-20} segment because of its higher tendency to form β-sheets than the Aβ_{18-24} segment. Finally, the calculation of distances during a 15 μs MD simulation of a 1:1 system of Aβ_{12-28} and Aib-1, compared to NOE distance restraints determined by NMR, indicated that most intramolecular long-range and intermolecular NOE upper distance limits were either satisfied or marginally violated (Supporting Information S6).

NMR-Derived Ensemble of Aib-1-Aβ_{12-28} Complex. A nonaggregative, truncated Aβ_{12-28} peptide was used in order to prevent spectral complications from kinetic oligomerization during acquisition. Aβ_{12-28} was added to a 4-fold molar excess of Aib-1, and spectra were acquired in the presence or absence of Aib-1 and assigned (Supporting Information Table 1 and S7). Deviations in backbone chemical shifts between the peptide

dx.doi.org/10.1021/cb200103h |*ACS Chem. Biol.* 2011, 6, 1265–1276

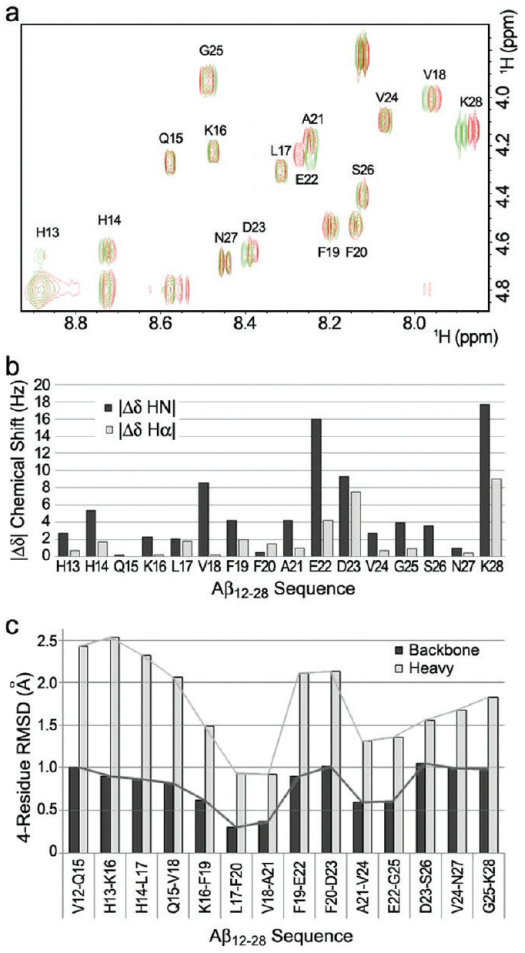

Figure 6. Changes in Aβ_{12-28} NMR chemical shifts upon binding Aib-1. (a) HN-Hα region of the TOCSY spectra of Aβ_{12-28} alone (red) and bound to Aib-1 with a 1:4 ratio (green) showing strong deviations in Val18, Glu22, and Asp23 and the terminal residues. (b) Chart of deviations in HN (black) and Hα (gray) chemical shift values upon binding. (c) Local 4-residue rmsd (Å) of Aβ_{12-28}: HN (black) and Hα (gray).

alone and with Aib-1 were seen at V18, F19, A21, E22, D23, and terminal residues (Figure 6a−c and Supporting Information Table 2). Aib-1 showed changes in chemical shift of over 4 Hz for all resolved protons and particularly high changes in W3 HN (17 Hz) and F4 Hβ (19 Hz) (Supporting Information Table 2). The three nonterminal residues, whose chemical shift values change most upon interacting with the Aib-1 inhibitor, are likely to participate in the interaction with the inhibitor.

The spectra afforded adequate data for structure determination (Table 1 and Supplementary Table 3); however, the structures obtained (Figure 7a−c) did not converge into any resolved conformation with a clear region of interaction with the ligand. The disordered ensemble of Aβ_{12-28} is consistent with a Monte Carlo simulation study of the monomeric Aβ_{1-40} and Aβ_{1-42} ensembles.[53] In contrast, Aib-1 gave a well-resolved conformation (Table 1, Figure 7d) with a low rmsd (0.3 Å for backbone atoms) and was found proximate to Aβ_{12-28} in a number of orientations. There were three intermolecular interactions found: between F20 Hε and Y1 Hε; A21 Hβ and W3 Hβ; and E22 Hα to both resolved Aib2 Hβ methyls, in Aβ_{12-28} and Aib-1, respectively (Supplementary Table 3). These indicated

Table 1

Restraints used in structure calculation
Total number of restraints – 201 Intra-residual restraints – 81 *i*+1 restraints – 84 *i*+2 restraints – 24 *i*+3 restraints – 7 Long range restraints – 1 Intermolecular restraints – 4
Ensemble statistics
Starting Ensemble of 50 Aβ_{12-28} Backbone RMSD 2.7 Å; Heavy atom RMSD 3.8 Å Aib-1 Backbone RMSD 0.7 Å; Heavy atom RMSD 1.4 Å
Ensemble of 28/50 non-violated Aβ_{12-28} Backbone RMSD 2.7 Å; Heavy atom RMSD 3.8 Å Aib-1 Backbone RMSD 0.5 Å; Heavy atom RMSD 1.2 Å
Presented ensemble of 10/28 Aβ_{12-28} Backbone RMSD 2.5 Å; Heavy atom RMSD 3.7 Å Aib-1 Backbone RMSD 0.3 Å; Heavy atom RMSD 0.8 Å

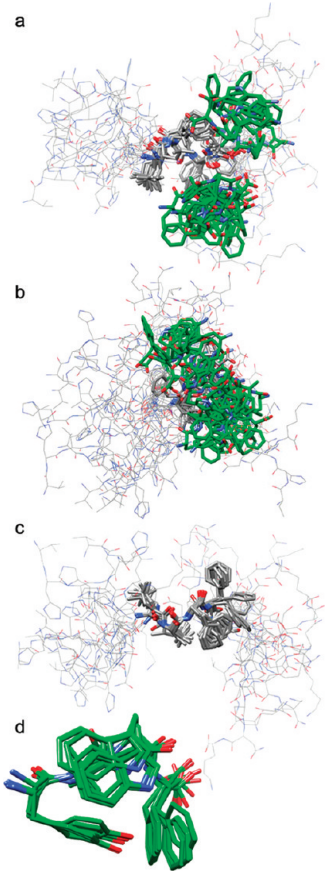

Figure 7. NMR-derived ensemble of Aβ_{12-28}-Aib-1 complex. Complex of Aβ_{12-28} (gray) and Aib-1 (green-stick presentation) superimposed over (a) residues 17−21 (stick representation) and (b) residues 20−22. (c) Different view of panel a showing Aβ_{12-28} only. (d) Aib-1 backbone superimposed ensemble.

hydrophobic, aromatic, and polar interactions between the molecules (Figure 7a,b). The transient interactions and those with F20 and E22 were consistent with the MD simulations of

dx.doi.org/10.1021/cb200103h |*ACS Chem. Biol.* 2011, 6, 1265–1276

the Aβ_{12-28} peptide with one molecule of Aib-1 (Figure 5). Moreover, the intermolecular NOE upper distance limits were mostly upheld during the MD simulations of Aβ_{12-28}/Aib-1 (Supporting Information S6). There were a number of hydrogen bonds between conformations of the Aβ_{12-28} and Aib-1 complex, but none was persistent and repeated in a number of members of the ensemble. A number of different interactions between Aib-1 and Aβ_{12-28} occur with almost equal probabilities, seen both by NOE interactions and within the complex ensemble. Possibly, the enhanced activity of Aib-1 is due to its ability to interact with Aβ_{12-28} *via* two additional modes, *i.e.*, hydrophobic and polar, in addition to the canonical aromatic one. The interaction of the Aib residue in Aib-1 with the hydrophobic patch on Aβ_{12-28} and the negatively charged E22 and D23 may explain why the chemical shifts of these residues change so much upon binding. This interaction may mask the aromatic residues, thereby preventing them from promoting aggregation.[11,12] The favorable interaction between the K16 side chain and Aib-1 in the MD simulations was not evident by NMR, probably due to fact that the amine moiety is in fast exchange with water and not detectable by NMR.

Conclusion. We conclude that there is a fundamental difference in the mode of activity of the native endomorphin peptide and its Aib-substituted analogues. The observation that a Pro to Aib substitution resulted in a major improvement of the inhibitory potential of the tetra-peptide is consistent with structural models showing the effect of an Aib residue on conformational flexibility. The experimental and simulation results of our study suggest a novel direction for developing inhibitors of amyloid formation, incorporating an Aib moiety as a β-breaker with enhanced hydrophobic properties. Further to the role of key aromatic residues in self-assembly processes such as amyloid formation, we demonstrate that the combination of a hydrophobic, β-structure-breaking Aib modification and an endogenous peptide (with three aromatic side chains) increased inhibition of Aβ peptide self-assembly.

METHODS

Aβ, Endomorphins, and Derivatives. Synthetic lyophilized Aβ_{1-40}, Aβ_{1-42} and Aβ_{12-28} were purchased from Bachem, Bubendorf, Switzerland. EM-1 and EM-2 were purchased from Sigma-Aldrich Inc. EM-1 and EM-2 were 99% pure by HPLC. Aib-1 and Aib-1 (D-amino acids) were synthesized by Peptron, Inc., South Korea by conventional solid-phase peptide synthesis. Aib-1 was 99% purified. The purified peptide was analyzed by HPLC using a Shiseido capcell pak C18 column and an acetonitrile gradient (A; 0.1% TFA water, B; 0.1% TFA acetonitrile) followed by HP 1100 series LC/MSD

Determination of Soluble Oligomer Formation. Aβ intermediates and toxic oligomers were produced according to Barghorn *et al.*[4] To avoid preaggregation, synthetic lyophilized Aβ_{1-42} was pretreated with 500 μL of 100% HFIP, sonicated for 20 s in ice−water, and incubated for 2 h at 37 °C under shaking at 100 rpm. After evaporation in a speedVac, Aβ_{1-42} was resuspended in dimethyl sulfoxide (DMSO) (with or without the inhibitors) to 5 mM and diluted with 20 mM NaH_2PO_4, 140 mM NaCl, pH 7.4 to a final concentration of 400 μM and 0.1 vol 2% SDS (final concentration of 0.2%). The Aβ toxic oligomers were generated by further dilution with 2 vol of H_2O and incubated for another 18 h. Aβ aggregation products were then separated using a 15% Tris-tricine gel and stained using Imperial protein stain and Western blot using antibody 6E10 (SIGNET).

Fluorescence Anisotropy Studies. EM-1 and Aib-1 were dissolved in DMSO to concentration of 0.5 μM and sonicated for 5 min. The solution was immediately mixed with aliquots of an Aβ_{1-42} intermediate (as described above) stock solution (20 μM/400 μM) to varying final polypeptide concentrations. EM-1 and Aib-1 polarization measurements were carried out using an ISS K2 fluorometer. The solutions were excited at 280 nm and emission was monitored at 350 nm. At least five measurements were collected for each point, and their average values were used for the calculation. All experiments were performed in ultrapure water.

ThT Binding Fluorescence. Synthetic lyophilized Aβ_{1-40} was dissolved in DMSO to a concentration of 100 μM and sonicated in ice−water for 20 s to prevent preaggregation. Aβ solutions were prepared by immediate dilution with 10 mM phosphate-buffered saline [100 mM NaCl and 0.5 mM EDTA (pH 7.4)] to a final concentration of 10 μM [containing 10% (v/v) DMSO]. A 10 μM Aβ_{1-42} solution was immediately mixed with the different inhibitors stock solutions (100 μM) to a final Aβ_{1-42} concentration of 5 μM and different inhibitor concentrations (1 μM up to 50 μM). The samples were incubated at 37 °C, and the fibrillogenesis rate was monitored using ThT fluorescence analysis. The respective excitation and emission wavelengths were 450 nm (2.5 nm slit) and 480 nm (5 nm slit). A 10-fold diluted sample was taken and mixed with 450 μL of 0.4 μM ThT. The fluorescence of ThT was measured using a Jobin Yvon Horiba Fluoromax 3 fluorimeter. Each experiment was repeated in quadruplicate.

Transmission Electron Microscopy. Samples (10 μL) from the ThT fluorescence assays were placed on 400 mesh copper grids covered by carbon-stabilized Formvar film (SPI Supplies, West Chester, PA). After 1.5 min, excess fluid was removed, and the grids were negatively stained with 10 μL of 2% uranyl acetate solution for 1.5 min. Finally, excess fluid was removed, and the samples were viewed in a JEOL 1200EX electron microscope operating at 80 kV.

Bacterial Fluorescence Screen for Inhibitors of Aβ Aggregation. The protocol established by Kim *et al.*[39] was used. Strain BL21 (DE3) *E. coli* cells harboring the Aβ_{42}-GFP fusion vector were grown in LB media supplemented with 50 μg/mL kanamycin. When cultures reached an OD_{600} of 0.8, 200 μL of culture were transferred to 96-well plates. Different concentrations of EM-1 and Aib-1 were added to each well, and protein expression was induced by adding isopropyl-β-D-thiogalactopyranoside to a final concentration of 1 mM. Samples were incubated with gentle agitation at 37 °C. Following 3 h of incubation, the fluorescence of each well was measured at 512 nm (excitation 490 nm) using an automated plate reader (Synergy HT Multi-Mode microplate Reader, BioTek). To verify that cell densities were consistent across all samples, the OD_{600} was also measured. Compounds were tested in triplicate at concentrations of 5, 50, and 100 μM. The identification of hits was consistent across several repetitions.

Cells Cytotoxicity Assay. A PC12 pheochromocytoma cell line was routinely grown in Dulbecco's Modified Eagle Medium (DMEM) supplemented with 8% fetal calf serum, 8% horse serum, 100 U/mL penicillin, 100 U/mL streptomycin, and 2 mM L-glutamine. Subconfluent cells were harvested by trypsinization, counted, diluted in the cell media to 2×10^4 cells/mL, then cultured in 96 well plates (100 μL/well) and incubated overnight at 37 °C. In order to exclude the effect of the serum, the wells were washed once with serum-free DMEM. Then, into each well was added 100 μL of DMEM with Aβ1-$_{42}$ fibrils 1 μM previously incubated with or without Aib-1 (as described above) or Aβ_{1-42} oligomers 5 μM that were incubated previously with or without Aib-1. The Aβ_{1-42} oligomers were first precipitated with acetone to exclude toxicity of the SDS and HFIP from the oligomer preparation protocol of Barghorn *et al.* Each treatment was performed in four repeats. After 24 h incubation at 37 °C, cell viability was evaluated using the thiazolyl-blue-tetrazolium-bromide (MTT) assay. Briefly, 10 μL of 10 mg/mL MTT dissolved in PBS was added into each well. After 4 h incubation at 37 °C, 100 μL of extraction buffer (20% SDS dissolved in 50% dimethylformamide and 50% DDW solution, pH 4.7) was added to

each well, and the plates were incubated again overnight at 37 °C. Finally, color intensity was measured using an ELISA Reader at 570 nm.

Cells viability (%) = OD (570 nm) in the presence of Aβ with or without inhibitor × 100, and O.D. (570 nm) when only inhibitor was added.

***In Vitro* Assay of Peptide Stability.** Peptides were prepared in a 1 mM solution in 50 mM Tris buffer (pH = 7.6), and 120 μL of the peptide solution was diluted in 10% freshly prepared mouse brain homogenate without the cerebellum (in 1X Tris buffer and 0.5% Triton X-100). A mixture containing 20% peptide solution and 80% mouse brain homogenate was incubated at 37 °C with delicate shaking for 2 h. The enzyme reaction was stopped by adding 0.1 M HCl solution, followed by denaturation of the protein using CH_3OH and incubation at 20 °C for 1 h. The precipitated proteins were centrifuged at 29,000 × *g* for 20 min at 4 °C, and the supernatant containing the peptide was concentrated under vacuum and separated using a C18 HPLC column. The area of the peak (UV absorbance at 280 nm) corresponding to the intact peptide was compared with an equivalent sample incubated in 50 μM Tris buffer.

Fly Keeping. Flies were reared on standard cornmeal-molasses medium and were kept at 25 °C. As *Drosophila* females can store sperm cells in their bodies, crosses were conducted using virgin females collected no longer than 8 h after eclosion at 25 °C or 18 h after eclosion at 18 °C. Adult offspring (F1) from the crosses were collected up to 9 days after the beginning of their eclosion at 25 °C in order to avoid offspring from the next generation (F2).

Fly Crossing. Female flies carrying the driver elav^{FM7}-Gal4 were crossed with males carrying the AβArc$_{-42}$ transgene (located on an autosome) under the UAS promoter in a homozygous condition. This resulted in first generation (F1) offspring expressing AβArc$_{-42}$ in their nervous system. They served as our Arc Alzheimer's *Drosophila* model. F1 offspring, which carried the AβArc$_{-42}$ transgene but did not express it (because they lacked the Gal4 driver) served as a control.

Longetivity Assay. Flies expressing AβArc$_{-42}$ reared at 29 °C on a medium with or without Aib-1 (D-amino acids) were separated to four classes: (1) F1 offspring expressing AβArc$_{-42}$, on regular medium; (2) F1 offspring expressing AβArc$_{-42}$, on medium supplemented with Aib-1; (3) F1 offspring controls (lacking the Gal4 driver) supplemented with Aib-1; and (4) F1 offspring controls (lacking the Gal4 driver) on regular medium. For each class, four plastic vials each with 15 flies were collected and fresh food was given every 3 days (with or without Aib-1). The number of viable AβArc$_{-42}$-expressing and control flies treated with and without Aib-1 was recorded daily post eclosion. Differences in survival rates were analyzed using the SPSS 11 Kaplan-Meir software package.

MD Simulation Protocol and Trajectory Analysis. Langevin dynamics simulations were used to investigate the aggregation of eight replicas of capped Aβ_{14-20} and Aβ_{18-24} peptidic segments in the presence and absence of one single Aib-1 molecule. The simulations were performed with the CHARMM program;[48,54] the peptides and compound were modeled using the united atoms CHARMM PARAM19 force field with its default truncation scheme for nonbonding interactions (cutoff of 7.5 Å). Protonation states of titratable residues were considered to be those at pH 7.0, and solvation effects were implicitly accounted for by using FACTS.[47] The non-polar solvation was approximated by a term proportional to the surface area with a multiplicative surface tension-like parameter of 0.0075 kcal/(mol·Å^2).

The simulations were prepared according to the protocol described by Convertino *et al.*[22] using eight monodispersed replicas of the same Aβ heptapeptide in the simulation box with zero or one uncapped Aib-1 molecule. In the latter case, the concentration ratio Aβ heptapeptide/compound was 8:1. The simulations were carried out with periodic boundary conditions at fixed peptide concentration of 4.88 mM (the simulations box was set to 132 Å), using Langevin integrator at low friction constant (0.15 ps^{-1}) and at the temperature of 27 °C. Ten independent simulations of 2.0 μs each were run for each of the four systems using different initial random velocities. In addition, three 5.0 μs runs were carried out for a system consisting of one Aβ_{12-28} peptide and one Aib-1 molecule to calculate NOE distance violations.

The influence of Aib-1 on the ordered aggregation of the octameric systems was measured by analyzing the average number of inter- and intrapeptide backbone H-bonds and their distributions for each studied system (Figure 4a−d in the main text). The hydrogen bond is defined by a distance threshold of 2.5 Å and a NH−O angle larger than 130°. All energy evaluations were carried out with CHARMM using the same force field as in the Langevin runs. Standard errors were estimated by block averaging. The 10 simulations were divided into two independent blocks of five runs each, and results for each block were plotted separately.

NMR Structure Determination. Samples were prepared by dissolving 1.4 mg of Aib-1 in lyophilized form in 90 μL of d_6-DMSO; this solution was added to 1.0 mg of lyophilized Aβ_{12-28} to which TDW with 0.02% w/v NaN_3 was added to obtain a final sample of 1.13 mM peptide with a 4:1 ratio of Aib-1 to peptide, in 20% d_6-DMSO solution. The reference sample without Aib-1 was prepared in exactly the same manner, without adding Aib-1. pH was titrated to 4.40 ± 0.05 with NaOH. The order of dissolving the peptide is essential to achieve solubility. NMR experiments were performed on a Bruker Avance 600 MHz DMX spectrometer operating at the proton frequency of 600.13 MHz, at 21.0 °C. The transmitter frequency was set to the water signal, which was calibrated at 4.811 ppm. Correlation spectroscopy (COSY),[55] total correlation spectroscopy (TOCSY)[56] using the MLEV-17 pulse scheme for the spin lock,[56] and nuclear Overhauser effect spectroscopy (NOESY)[57,58] experiments were acquired under identical conditions for all samples, using gradients for water saturation[59] and a mixing time of 160 ms. Spectra were processed and analyzed with TopSpin (Bruker Analytische Messtechnik GmbH) and SPARKY3 (Goddard, T. D., and Kneller, D. G., SPARKY 3, University of California, San Francisco) Software. Resonance assignment followed the sequential assignment methodology developed by Wüthrich.[60] Peak intensities were manually assigned from the van der Waals radius up to strong (2.5 Å), medium (3.5 Å), weak (4.5 Å), and very weak (5.5 Å). The three-dimensional structures of the peptides were calculated using XPLOR (version 3.856)[61] by hybrid distance geometry-dynamical simulated annealing. The Aib-1 residue was introduced using patches within XPLOR. Fifty initial structures were generated by simulated annealing. The NOE energy was introduced as a square-well potential. Molmol[62] was used to create the final ensemble of structures. Low energy structures chosen for further analysis had no NOE violations, deviations from ideal bond lengths of less than 0.05 Å, and bond angle deviations from ideality of less than 5°. Figures were made using Chimera.[63]

■ ASSOCIATED CONTENT

Supporting Information. This material is available free of charge *via* the Internet at http://pubs.acs.org.

■ AUTHOR INFORMATION

Corresponding Author

*E-mail: ehudg@post.tau.ac.il; deborah.shalev@huji.ac.il; caflisch@bioc.uzh.ch.

■ ACKNOWLEDGMENT

We wish to thank Yaacov Delarea for help with electron microscopy experiments, Prof. Michael Hecht for supplying us with the GFP-Aβ system, Aviad Levin for help with the pape, and members of the Gazit laboratory for helpful discussions. Part of this work was supported financially by a Swiss National Science Foundation grant to A.C.

ABBREVIATIONS

Aβ, β-amyloid polypeptide; AD, Alzheimer's disease; ADDLs, amyloid-derived diffusible ligands; Aib, α-aminoisobutyric acid; COSY, correlation spectroscopy; DMEM, Dulbecco'S Modified Eagle Medium; DMSO, dimethyl sulfoxide; E22G, the arctic (Arc) mutant form of Aβ; EM-1, endomorphin-1 (Tyr-Pro-Trp-Phe); EM-2, endomorphin-2 (Tyr-Pro-Phe-Phe); GFP, green fluorescence protein; HFIP, hexafluoro-2-propanol; HPLC, high performance liquid chromatography; IPTG, isopropyl-β-D-thiogalactopyranoside; MD, molecular dynamics; MTT, thiazolyl-blue-tetrazolium-bromide; NMR, nuclear magnetic resonance; NOESY, nuclear overhauser effect spectroscopy; TEM, transmission electron microscopy; ThT, thioflavin-T; TOCSY, total correlation spectroscopy

REFERENCES

(1) Querfurth, H. W., and LaFerla, F. M. (2010) Alzheimer's disease. *N. Engl. J. Med. 362*, 329–344.

(2) Bharadwaj, P. R., Dubey, A. K., Masters, C. L., Martins, R. N., and Macreadie, I. G. (2009) Abeta aggregation and possible implications in Alzheimer's disease pathogenesis. *J. Cell. Mol. Med. 13*, 412–421.

(3) Bertram, L., Lill, C. M., and Tanzi, R. E. (2010) The genetics of Alzheimer disease: back to the future. *Neuron 68*, 270–281.

(4) Barghorn, S., Nimmrich, V., Striebinger, A., Krantz, C., Keller, P., B., J., Bahr, M., Schmidt, M., Bitner, R. S., Harlan, J., Barlow, E., Ebert, U., and Hillen, H. (2005) Globular amyloid beta-peptide oligomer − a homogenous and stable neuropathological protein in Alzheimer's disease. *J. Neurochem. 95*, 834–847.

(5) Lesne, S., Koh, M., Kotilinek, T., Kayed, L., Glabe, R., C., G., Yang, A., Gallagher, M., and Ashe, K. H. (2006) A specific amyloid−β protein assembly in the brain impairs memory. *Nature 440*, 352–357.

(6) Catalano, S. M., Dodson, E. C., Henze, D. A., Joyce, J. G., Krafft, G. A., and Kinney, G. G. (2006) The role of amyloid-beta derived diffusible ligands (ADDLs) in Alzheimer's disease. *Curr. Top. Med. Chem. 6*, 597–608.

(7) Lambert, M. P., Barlow, A. K., Chromy, B. A., Edwards, C., Freed, R., Liosatos, M., Morgan, T. E., Rozovsky, I., Trommer, B., Viola, K. L., Wals, P., Zhang, C., Finch, C. E., Krafft, G. A., and Klein, W. L. (1998) Diffusible, nonfibrillar ligands derived from Aβ1−42 are potent central nervous system neurotoxins. *Proc. Natl. Acad. Sci. U.S.A.* 6448–6453.

(8) Gazit, E. (2005) Mechanisms of amyloid fibril self-assembly and inhibition. Model short peptides as a key research tool. *FASEB J. 272*, 5971–5978.

(9) Gazit, E. (2002) A possible role for π-stacking in self-assembly of amyloid fibrils. *FASEB J. 16*, 77–83.

(10) Azriel, R., and Gazit, E. (2001) Analysis of the minimal amyloid-forming fragment of the islet amyloid polypeptide. an experimental support for the key role of the phenylalanine residue in amyloid formation. *J. Biol. Chem. 276*, 34156–34161.

(11) Makin, O. S., Atkins, E., Sikorski, P., Johansson, J., and Serpell, L. C. M. (2005) Molecular basis for amyloid fibril formation and stability. *Proc. Natl. Acad. Sci. U.S.A. 102*, 315–320.

(12) Inouye, H., Sharma, D., Goux, W. J., and Kirschner, D. A. (2006) Structure of core domain of fibril forming PHF/Tau fragments. *Biophys. J. 90*, 1774–1789.

(13) Platt, G. W., Routledge, K. E., Homans, S. W., and Radford, S. E. (2008) Fibril growth kinetics reveal a region of beta2-microglobulin important for nucleation and elongation of aggregation. *J. Mol. Biol. 378*, 251–263.

(14) Buyong Ma, and Nussinov, R. (2007) Trp/Met/Phe hot spots in protein-protein interactions: potential targets in drug design. *Curr. Top. Med. Chem. 7*, 999–1005.

(15) Pawar, A. P., Dubay, K. F., Zurdo, J., Chiti, F., Vendruscolo, M., and Dobson, C. M. (2005) Prediction of "aggregation-prone" and "aggregation susceptible" regions in proteins associated with neurodegenerative diseases. *J. Mol. Biol. 350*, 379–392.

(16) Frydman-Marom, A., Rechter, M., Shefler, I., Bram, Y., Shalev, D. E., and Gazit, E. (2009) Cognitive-performance recovery of Alzheimer's disease model mice by modulation of early soluble amyloidal assemblies. *Angew. Chem., Int. Ed. 48*, 1981–1986.

(17) Kokkoni, N., Stott, K., Amijee, H., Mason, J. M., and Doig, A. J. (2006) N-Methylated peptide inhibitors of beta-amyloid aggregation and toxicity. Optimization of the inhibitor structure. *Biochemistry 45*, 9906–9918.

(18) Etienne, M. A., Aucoin, J. P., Fu, Y., McCarley, R. L., and Hammer, R. P. (2006) Stoichiometric inhibition of amyloid beta-protein aggregation with peptides containing alternating alpha,alpha-disubstituted amino acids. *J. Am. Chem. Soc. 128*, 3522–3523.

(19) Porat, Y., Abramowitz, A., and Gazit, E. (2006) Inhibition of amyloid fibril formation by polyphenols: Structural similarity and aromatic interactions as a common. *Chem. Biol. Drug Des.* 27–37.

(20) Cohen, T., Frydman-Marom, A., Rechter, M., and Gazit, E. (2006) Inhibition of amyloid fibril formation and cytotoxicity by hydroxyindole derivatives. *Biochemistry 45*, 4727–4735.

(21) Scherzer-Attali, R., Pellarin, R., Convertino, M., Frydman-Marom, A., Egoz-Matia, N., Peled, S., Levy-Sakin, M., Shalev, D. E., Caflisch, A., Gazit, E., and Segal, D. (2010) Complete phenotypic recovery of an Alzheimer's disease model by a quinone-tryptophan hybrid aggregation inhibitor. *PLoS One 5*, e11101.

(22) Convertino, M., Pellarin, R., Catto, M., Carotti, A., and Caflisch, A. (2009) 9,10-Anthraquinone hinders beta-aggregation: how does a small molecule interfere with Abeta-peptide amyloid fibrillation? *Protein Sci. 18*, 792–800.

(23) Soto, C., Sigurdsson, E. M., Morelli, L., Kumar, R. A., Castaño, E. M., and Frangione, B. (1998) β-sheet breaker peptides inhibit fibrillogenesis in a rat brain model of amyloidosis: Implications for Alzheimer's therapy. *Nat. Med. 4*, 822–826.

(24) Gilead, S., and Gazit, E. (2004) Inhibition of amyloid fibril formation by peptide analogues modified with alpha-aminoisobutyric acid. *Angew. Chem., Int. Ed. 43*, 4041–4044.

(25) Fichna, J., Janecka, A., Costentin, J., and Do Rego, J. C. (2007) The endomorphin system and its evolving neurophysiological role. *Pharmacol. Rev. 59*, 88–123.

(26) Hsiao, K., Chapman, P., Nilsen, S., Eckman, C., Harigaya, Y., Younkin, S., Yang, F., and Cole, G. (1996) Correlative memory deficits, Abeta elevation, and amyloid plaques in transgenic mice. *Science 274*, 99–102.

(27) Chacon, M. A., Barria, M. I., Soto, C., and Inestrosa, N. C. (2004) Beta-sheet breaker peptide prevents Abeta-induced spatial memory impairments with partial reduction of amyloid deposits. *Mol. Psychiatry 9*, 953–961.

(28) Szegedi, V., Juhasz, G., Rozsa, E., Juhasz-Vedres, G., Datki, Z., Fulop, L., Bozso, Z., Lakatos, A., Laczko, I., Farkas, T., Kis, Z., Toth, G., Soos, K., Zarandi, M., Budai, D., Toldi, J., and Penke, B. (2006) Endomorphin-2, an endogenous tetrapeptide, protects against Abeta1−42 in vitro and in vivo. *FASEB J. 20*, 1191–1193.

(29) Roher, A. E., Lowenson, J. D., Clarke, S., Woods, A. S., Cotter, R. J., Gowing, E., and Ball, M. J. (1993) beta-Amyloid-(1−42) is a major component of cerebrovascular amyloid deposits: implications for the pathology of Alzheimer disease. *Proc. Natl. Acad. Sci. U.S.A. 90*, 10836–10840.

(30) Porat, Y., Stepensky, A., Ding, F. X., Naider, F., and Gazit, E. (2003) Completely different amyloidogenic potential of nearly identical peptide fragments. *Biopolymers 69*, 161–164.

(31) Porat, Y., Mazor, Y., Efrat, S., and Gazit, E. (2004) Inhibition of Islet amyloid polypeptide fibril formation: a potential role for heteroaromatic interactions. *Biochemistry 43*, 14454–14462.

(32) Karle, I. L., and Balaram, P. (1990) Structural characteristics of alpha-helical peptide molecules containing Aib residues. *Biochemistry 29*, 6747–6756.

(33) Formaggio, F., Bettio, A., Moretto, V., Crisma, M., Toniolo, C., and Broxterman, Q. B. (2003) Disruption of the beta-sheet structure of a protected pentapeptide, related to the beta-amyloid sequence 17−21, induced by a single, helicogenic C(alpha)-tetrasubstituted alpha-amino acid. *J. Pept. Sci. 9*, 461–466.

(34) Kim, H. J., Chae, S. C., Lee, D. K., Chromy, B., Lee, S. C., Park, Y. C., Klein, W. L., Krafft, G. A., and Hong, S. T. (2003) Selective neuronal degeneration induced by soluble oligomeric amyloid beta protein. *FASEB J. 17*, 118–120.

(35) Gazit, E. (2004) The role of prefibrillar assemblies in the pathogenesis of amyloid diseases. *Drugs Future 29*, 613–619.

(36) Klein, W. L., Krafft, G. A., and Finch, C. E. (2001) Targeting small Abeta oligomers: the solution to an Alzheimer's disease conundrum? *Trends Neurosci. 24*, 219–224.

(37) De Felice, F. G., Vieira, M. N., Saraiva, L. M., Figueroa-Villar, J. D., Garcia-Abre, J., Liu, R., Chang, L., Klein, W. L., and Ferreira, S. T. (2004) Targeting the neurotoxic species in Alzheimer's disease: inhibitors of A beta oligomerization. *FASEB J. 18*, 1366–1372.

(38) Frydman-Marom, A., Levin, A., Farfara, D., Benromano, T., Scherzer-Attali, R., Peled, S., Vassar, R., Segal, D., Gazit, E., Frenkel, D., and Ovadia, M. (2011) Orally administrated cinnamon extract reduces beta-amyloid oligomerization and corrects cognitive impairment in Alzheimer's disease animal models. *PLoS One 6*, e16564.

(39) Kim, W., Kim, Y., Min, J., Kim, D. J., Chang, Y. T., and Hecht, M. H. (2006) A high-throughput screen for compounds that inhibit aggregation of the Alzheimer's peptide. *ACS Chem. Biol. 1*, 461–469.

(40) Cubitt, A. B., Heim, R., Adams, S. R., Boyd, A. E., Gross, L. A., and Tsien, R. Y. (1995) Understanding, improving and using green fluorescent proteins. *Trends Biochem. Sci. 20*, 448–455.

(41) Wurth, C., Guimard, N. K., and Hecht, M. H. (2002) Mutations that reduce aggregation of the Alzheimer's Abeta42 peptide: an unbiased search for the sequence determinants of Abeta amyloidogenesis. *J. Mol. Biol. 319*, 1279–1290.

(42) Adessi, C., and Soto, C. (2002) Converting a peptide into a drug: strategies to improve stability and bioavailability. *Curr. Med. Chem. 9*, 963–978.

(43) Yamaguchi, H., Kodama, H., Osada, S., Kato, F., Jelokhani-Niaraki, M., and Kondo, M. (2003) Effect of alpha,alpha-dialkyl amino acids on the protease resistance of peptides. *Biosci. Biotechnol. Biochem. 67*, 2269–2272.

(44) Shaltiel-Karyo, R., Frenkel-Pinter, M., Egoz-Matia, N., Frydman-Marom, A., Shalev, D. E., Segal, D., and Gazit, E. (2010) Inhibiting alpha-synuclein oligomerization by stable cell-penetrating beta-synuclein fragments recovers phenotype of Parkinson's disease model flies. *PLoS One 5*, e13863.

(45) Crowther, D. C., KIinghorn, K. J., Miranda, E., Page, R., Curry, J. A., Duthie, F. A. I., Gubb, D. C., and Lomas, D. A. (2005) Intraneuronal Aβ, non-amyloid aggregates and neurodegeneration in a Drosophila model of Alzheimer's disease. *Neuroscience 132*, 123–135.

(46) Nilsberth, C., Westlind-Danielsson, A., Eckman, C. B., Condron, M. M., Axelman, K., Forsell, C., Stenh, C., Luthman, J., Teplow, D. B., Younkin, S. G., Naslund, J., and Lannfelt, L. (2001) The 'Arctic' APP mutation (E693G) causes Alzheimer's disease by enhanced Abeta protofibril formation. *Nat. Neurosci. 4*, 887–893.

(47) Haberthur, U., and Caflisch, A. (2008) FACTS: Fast analytical continuum treatment of solvation. *J. Comput. Chem. 29*, 701–715.

(48) Brooks, B. R., Brooks, C. L., 3rd, Mackerell, A. D., Jr., Nilsson, L., Petrella, R. J., Roux, B., Won, Y., Archontis, G., Bartels, C., Boresch, S., Caflisch, A., Caves, L., Cui, Q., Dinner, A. R., Feig, M., Fischer, S., Gao, J., Hodoscek, M., Im, W., Kuczera, K., Lazaridis, T., Ma, J., Ovchinnikov, V., Paci, E., Pastor, R. W., Post, C. B., Pu, J. Z., Schaefer, M., Tidor, B., Venable, R. M., Woodcock, H. L., Wu, X., Yang, W., York, D. M., and Karplus, M. (2009) CHARMM: the biomolecular simulation program. *J. Comput. Chem. 30*, 1545–1614.

(49) Williams, A. D., Portelius, E., Kheterpal, I., Guo, J. T., Cook, K. D., Xu, Y., and Wetzel, R. (2004) Mapping abeta amyloid fibril secondary structure using scanning proline mutagenesis. *J. Mol. Biol. 335*, 833–842.

(50) Cecchini, M., Curcio, R., Pappalardo, M., Melki, R., and Caflisch, A. (2006) A molecular dynamics approach to the structural characterization of amyloid aggregation. *J. Mol. Biol. 357*, 1306–1321.

(51) Tartaglia, G. G., Cavalli, A., Pellarin, R., and Caflisch, A. (2005) Prediction of aggregation rate and aggregation-prone segments in polypeptide sequences. *Protein Sci. 14*, 2723–2734.

(52) Gsponer, J., Haberthur, U., and Caflisch, A. (2003) The role of side-chain interactions in the early steps of aggregation: Molecular dynamics simulations of an amyloid-forming peptide from the yeast prion Sup35. *Proc. Natl. Acad. Sci. U.S.A. 100*, 5154–5159.

(53) Vitalis, A., and Caflisch, A. (2010) Micelle-like architecture of the monomer ensemble of Alzheimer's amyloid-beta peptide in aqueous solution and its implications for Abeta aggregation. *J. Mol. Biol. 403*, 148–165.

(54) Brooks, B. R., Bruccoleri, R. E, Olafson, B. D., States, D. J., and Swaminathan, S. (1983) CHARMM: A program for macromolecular energy, minimization, and dynamics calculations. *J. Comput. Chem.* 187–217.

(55) Aue, W. P., Bartholdi, E., and Ernst, R. R. (1976) Two dimensional spectroscopy. Application to nuclear magnetic resonance. *J. Chem. Phys. 64*, 2229–2246.

(56) Bax, A. D., and Davis, D. G. (1985) MLEV-17 based two-dimensional homonuclear magnetization transfer spectroscopy. *J. Magn. Reson.* 355–360.

(57) Jeener, J., Meier, B. H., Bachmann, P., and Ernst, R. R. (1979) Investigation of exchange processes by two dimensional NMR spectroscopy. *J. Chem. Phys. 71*, 4546–4553.

(58) Kumar, A., Ernst, R. R., and Wuthrich, K. (1980) A two-dimensional nuclear Overhauser enhancement (2D NOE) experiment for the elucidation of complete proton-proton cross-relaxation networks in biological macromolecules. *Biochem. Biophys. Res. Commun. 95*, 1–6.

(59) Liu, M., Mao, X., He, C., Huang, H., Nicholson, J. K., and Lindon, J. C. (1998) Improved WATERGATE pulse sequences for solvent suppression in NMR spectroscopy. *J. Magn. Reson. 132*, 125–129.

(60) Wüthrich, K. (1986) *NMR of Proteins and Nucleic Acids*, John Wiley & Sons, New York.

(61) Nilges, M., Kuszewski, J., Brunger, A. T. (1991) in *Computational Aspects of the Study of Biological Macromolecules by NMR* (Hoch, J. C., Ed.), New York: Plenum Press.

(62) Koradi, R., Billeter, M., and Wüthrich, K. (1996) MOLMOL: A program for display and analysis of macromolecular structures. *J. Mol. Graphics 14*, 51–55.

(63) Pettersen, E. F., Goddard, T. D., Huang, C. C., Couch, G. S., Greenblatt, D. M., Meng, E. C., and Ferrin, T. E. (2004) UCSF Chimera—a visualization system for exploratory research and analysis. *J. Comput. Chem. 25*, 1605–1612.

NOTE ADDED AFTER ASAP PUBLICATION

This article was published ASAP on September 19, 2011. The scale bar description has been updated in the legend of both Figure 1 and Figure 2. The corrected version was posted on October 3, 2011.